

Magnetostriction in Cubic Néel Ferrimagnets, with Application to YIG

E. R. CALLEN, A. E. CLARK, B. DESAVAGE, AND W. COLEMAN
U. S. Naval Ordnance Laboratory, White Oak, Silver Spring, Maryland

AND

H. B. CALLEN*

Laboratory for Research on the Structure of Matter, University of Pennsylvania, Philadelphia, Pennsylvania
 (Received 25 January 1963)

The magnetostriction of single-crystal yttrium iron garnet (YIG) has been measured from 100 to 450°K by a capacitive technique in which the sample dilatation shifts the resonant frequency of an oscillator, and by standard strain gauge methods. To analyze the data, the theory of magnetostriction in cubic insulators is applied to the Néel model of a ferrimagnet. This theory permits evaluation of the individual magnetoelastic coupling coefficients for each type of site (or sublattice) and for each symmetry of strain mode. The values found are $B_{0,2\gamma}(a) = -9.70 \times 10^6$ ergs/cm³, $B_{0,2\gamma}(d) = 8.95 \times 10^6$ ergs/cm³, $B_{0,2\epsilon}(a) = 5.67 \times 10^6$ ergs/cm³, $B_{0,2\epsilon}(d) = -17.2 \times 10^6$ ergs/cm³, where a and d refer to octahedrally and tetrahedrally coordinated sites, respectively, and γ and ϵ refer to linear dilatations and shear modes, respectively; the subscripts on the coefficients indicate that these are the coefficients of the lowest order symmetry polynomials, the higher order terms being found experimentally to be relatively small. Appropriate averaging of the above constants give "effective" constants in good agreement with the mean values found by other investigators. The theoretical predictions of the temperature dependence of the magnetostriction constants h_1 and h_2 are in excellent agreement with the observed values of h_1 , which has a minimum ($\sim -2.1 \times 10^{-8}$) near room temperature, and of h_2 which increases monotonically toward zero with increasing temperature.

I. INTRODUCTION

IN this paper we present experimental data on the magnetostriction of yttrium iron garnet (YIG) over a wide temperature range, and we apply the previously derived theory of magnetostriction in cubic insulators to the Néel model of a ferrimagnet. The theory and experiment are found to be consistent, permitting an excellent fit of the observed temperature dependence of the magnetostriction constants. This fit yields values of the individual magnetoelastic coupling coefficients for ions in each specific type of site, with each particular symmetry of strain mode. It is, of course, these single-ion coupling constants which are amenable to direct analysis by crystal field theory.

In simple ferromagnets the magnetostriction can be written as a function of the magnetization, as has been noted by Kittel and Van Vleck,¹ and as has been analyzed in specific detail by two of the authors in a paper² hereinafter to be referred to as I. In a ferrimagnet the magnetizations of the several sublattices may have different temperature dependences, and the resultant magnetostriction curves may, thereby, show fairly complicated forms. As one might expect, the magnetostriction is the net result of the magnetoelastic couplings of the separate magnetic sublattices to the crystal strain, each contribution to the strain depending on the sublattice magnetization by the familiar $l(l+1)/2$ law at low temperatures and by the corresponding spherical Bessel function dependence at higher temperatures.³ The theory, therefore, allows the relatively com-

plicated experimental temperature dependence of the magnetostriction to be unraveled, and thereby yields the separate underlying magnetoelastic coupling constants. Over the entire temperature range the theoretical curves agree with our experimental data for both $-h_1(T)$, which rises to a maximum near room temperature, and for $-h_2(T)$, which falls monotonically with rising temperature.

Consider the case of several sublattices, which we number $n = 1, 2 \dots$. Then the Hamiltonian is the sum of magnetic interactions H_m , the elastic energy H_e , the anisotropy energy H_a , and the magnetoelastic energy H_{me} . The first three terms are given explicitly in I; the magnetoelastic energy is assumed to be the sum of terms for each sublattice

$$H_{me} = \sum_n H_{me}(n). \quad (1)$$

Each term $H_{me}(n)$ is written in terms of phenomenological magnetoelastic coupling coefficients, precisely as in I, where we need merely add the sublattice index;

$$H_{me}(n) = - \sum_{\mu} \sum_{j,l} B_{j,l}^{\mu}(n) \sum_i \epsilon_i^{\mu,j} \mathcal{K}_i^{\mu,l}(n). \quad (2)$$

Here μ labels the irreducible representation (of which only five are permitted), j labels the strain modes of the μ th representation, i labels the functions which generate the μ th representation (so that i goes from unity to the dimensionality of Γ_{μ}), and l labels the degree of the spin operators. The quantity $\epsilon_i^{\mu,j}$ is then the amplitude of the i th strain component in the j th mode set which transforms under Γ_{μ} . $\mathcal{K}_i^{\mu,l}(n)$ is a Tensor Cubic Operator (TKO); a spin operator of the l th degree in the basic spin operators S_x, S_y, S_z , the set $\mathcal{K}_1^{\mu,l}, \mathcal{K}_2^{\mu,l} \dots$ transforming as Γ_{μ} . In the term with a given n the TKO depends on the spin operators of a lattice site of the n th sublattice.

* Supported by the Office of Naval Research.

¹ C. Kittel and J. H. Van Vleck, Phys. Rev. **118**, 1231 (1960).

² Earl R. Callen and Herbert B. Callen, Phys. Rev. **129**, 578 (1963).

³ E. R. Callen and H. B. Callen, J. Phys. Chem. Solids **16**, 310 (1960).

At a slightly more fundamental level, in which the terms of the Hamiltonian refer to the individual ions rather than to the sublattices, terms of lower symmetry than cubic appear. However, the summation over the various sites making up the given sublattice so combine⁴ these terms as to lead to a net Hamiltonian of cubic symmetry.

Minimizing the free energy with respect to the strains we obtain a solution completely analogous to that of I.

$$\epsilon_i^{\mu,i} = \frac{1}{c_j^\mu} \sum_l B_{j,l}^\mu(n) \langle Y_{l(\zeta)}^0(n) \rangle K_i^{\mu,l}(\zeta_n). \quad (3)$$

Here $K_i^{\mu,l}(\zeta_n)$ is a cubic harmonic (the classical analog of the TKO) which depends on the direction of the sublattice magnetization ζ_n . The quantity $\langle Y_{l(\zeta)}^0(n) \rangle$ is the average value in the unperturbed density matrix of the spherical tensor operator of degree l and order zero.

In the Néel model all sublattice magnetization directions $\zeta(n)$ are coaxial. Furthermore, for those TKOs permitted by time-reversal symmetry, $\langle \mathcal{K}_i^{\mu,l}(n) \rangle$ depends only on the axis of $\zeta(n)$ and not on its direction; hence, this quantity is independent of the sublattice index n . Then

$$\epsilon_i^{\mu,i} = \frac{1}{c_j^\mu} \sum_l \bar{B}_{j,l}^\mu(T) K_i^{\mu,l}(\zeta), \quad (4)$$

where

$$\bar{B}_{j,l}^\mu(T) = \sum_n B_{j,l}^\mu(n) \langle Y_{l(\zeta)}^0(n) \rangle. \quad (5)$$

Equation (4) is identical to that obtained in I, but the temperature dependence of the $\bar{B}_{j,l}(T)$, as determined by Eq. (5), may be more complicated, of course.

At low temperatures the average value $\langle Y_{l(\zeta)}^0(n) \rangle$ is equal to the $l(l+1)/2$ power of the sublattice magnetization, precisely as in the ferromagnetic case⁵:

$$\langle Y_{l(\zeta)}^0(n) \rangle = m_n^{l(l+1)/2}, \quad T \ll T_c, \quad (6)$$

whence

$$\bar{B}_{j,l}^\mu(T) = \sum_n B_{j,l}^\mu(n) m_n^{l(l+1)/2}. \quad (7)$$

At higher temperatures the $l(l+1)/2$ power law is not valid. However, we have calculated³ the classical average $\langle Y_{l(\zeta)}^0 \rangle$ in the internal field approximation, obtaining the result

$$\langle Y_{l(\zeta)}^0 \rangle = \frac{I_{l+1/2}(\mathcal{L}^{-1}(m_0))}{I_{1/2}(\mathcal{L}^{-1}(m_0))} \equiv \hat{I}_{l+1/2}(\mathcal{L}^{-1}(m_0)), \quad (8)$$

where I_l is the hyperbolic Bessel function and \mathcal{L}^{-1} is the inverse of the Langevin function. Equation (8) reduces to the $l(l+1)/2$ power law as m_0 approaches

⁴ This combination can be shown most readily by reducing the full cubic group according to the site symmetry, and by labeling the site functions in terms of their cubic parentage. Summation over the various equivalent sites, related to each other by the operations of the cubic group, then immediately couples the site functions to restore cubic symmetry.

⁵ J. H. Van Vleck, J. Phys. Radium 20, 128 (1959).

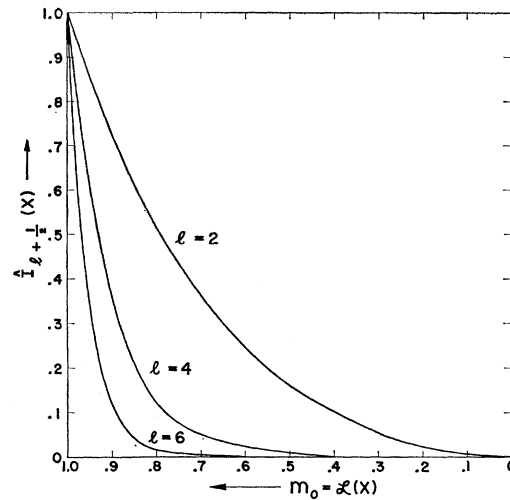


FIG. 1. Reduced hyperbolic Bessel functions $\hat{I}_{l+1/2}(x)$ vs reduced magnetization, $m_0 = \mathcal{L}(x)$, for $l=2, 4, 6$.

unity. The argument of the hyperbolic Bessel function, $\mathcal{L}^{-1}(m_0)$, has the physical significance of $\mu H_{\text{int}}/kT$, where μ is the magnetic moment of a site and H_{int} is the molecular field which acts on it. This field is actually a function of the sublattice magnetizations of other sublattices, but when written in the form of Eq. (8) the result can be applied to each sublattice simply by interpreting m_0 as the resultant magnetization m_n of that sublattice. All the underlying coupling of the sublattices are implicit in that they have, in effect, already determined m_n . Hence,

$$\bar{B}_{j,l}^\mu(T) = \sum_n B_{j,l}^\mu(n) \hat{I}_{l+1/2}(\mathcal{L}^{-1}(m_n)). \quad (9)$$

In Fig. 1 we plot $\hat{I}_{l+1/2}(\mathcal{L}^{-1}(m_0))$ as a function of m_0 for $l=2, 4, 6$. With these plots, and with the sublattice magnetizations, m_n , known either from the susceptibility using the Néel theory or by some other means (nuclear magnetic resonance, Mössbauer effect, neutron diffraction), one can then obtain the temperature dependences of the effective magnetoelastic coupling constants directly.

Although Eq. (4) for the strains is applicable to all the $k=0$ (infinite wavelength) strain modes, both acoustic and optical, in this paper we are only concerned directly with the *external* strains, those signified by $j=0$ in our notation. These are the strains which are measured as the external magnetostriction. The magnetostriction constants are defined by

$$\frac{\delta l}{l} = h_1 \sum_i \zeta_i^2 \xi_i^2 + 2h_2 (\zeta_1 \zeta_2 \xi_1 \xi_2 + \text{c.p.}) + \dots, \quad (10)$$

where ζ_i and ξ_i are the direction cosines of the magnetization and of the measurement direction, respectively. From reference I we recall that the magnetoelastic coupling coefficients are related to the magnetostriction

constants by

$$h_1(T) = \frac{3}{2}\lambda_{100} = C_1$$

$$\cong \frac{1}{c_{11}(T) - c_{12}(T)} \frac{15}{2 \times (4\pi)^{1/2}} \bar{B}_{0,2}{}^\gamma(T), \quad (11a)$$

$$h_2(T) = \frac{3}{2}\lambda_{111} = \frac{1}{2}C_2 \cong \frac{1}{2c_{44}(T)} \left(\frac{15}{4\pi}\right)^{1/2} \bar{B}_{0,2}{}^\epsilon(T). \quad (11b)$$

Because the polynomials of Eq. (10) are not orthogonal, they mix the various Kubic harmonics. This orthogonality is the advantage of the magnetostriction coefficients described in reference I. However, it will turn out that in the particular case of YIG there appear to be no higher order terms of substantial magnitude in Eq. (10), and Eq. (11) is accurate to within 5%. Consequently, knowing the temperature dependences of the sublattice magnetizations and of the elastic constants (which have only a slight temperature dependence) we can compare the experimentally determined magnetostriction constants with those found by means of Eq. (11), in which we adjust the coefficients $B_{0,2}{}^\mu(n)$ to obtain the best agreement.

Yttrium iron garnet is a simple Néel ferrimagnet, to which the above theory should apply directly. It contains two magnetic sublattices, with iron ions, respectively, on octahedral "a" sites and tetrahedral "d" sites. Consequently, there are just two adjustable coefficients (one for each sublattice) for each of the measured magnetostriction coefficients.

II. MAGNETOSTRICTION OF YIG, EXPERIMENTAL

The temperature dependences of the saturation magnetostriction constants, h_1 and h_2 , of YIG were measured over the temperature range from liquid nitrogen to 450°K. The sample, a 0.250-in. sphere, grown by Nielson,⁶ was prepared with four flat surfaces cut along the [001], [00 $\bar{1}$], [110], and [$\bar{1}\bar{1}$ 0] directions.

Standard strain gauge techniques, introduced by Goldman,⁷ were used to measure the temperature dependence of h_2 over the entire temperature range and the temperature dependence of h_1 above room temperature. This method is schematically represented by Fig. 2(b). Two strain gauges were mounted side by side; one on the YIG crystal, R_s , and the other on a dummy sample, R_d . The gauges were, then, connected as part of a Wheatstone bridge with large adjustable resistances R_s' and R_d' in parallel with R_s and R_d . If the change in resistance of the active gauge due to the strain of the sample is compensated for by changing R_s' , the magnetostriction is given by

$$\lambda = R_s \Delta R_s' / (R_s')^2 F, \quad (12)$$

where $\Delta R_s'$ is the change in R_s' and F is the gauge factor.

⁶ J. W. Nielson, Airtron Inc., Morris Plains, New Jersey.

⁷ J. E. Goldman, Phys. Rev. **72**, 529 (1947).

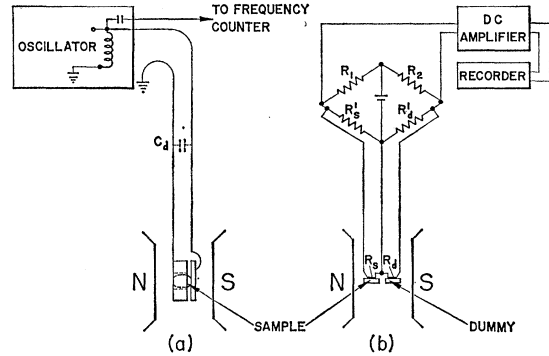


FIG. 2. Schematic diagrams of methods used to measure magnetostriction. (a) Capacitative method; (b) compensated strain gauge method.

Unfortunately, the method has the disadvantage that at low temperatures the change in magnetoresistance of the strain gauges with magnetic field orientation becomes large and not reproducible from one gauge to another. It is not unreasonable to have a pseudostrain of $\sim 0.4 \times 10^{-6}$ with these gauges at low temperatures. A more direct method, although somewhat more difficult because of bonding techniques, was used to measure the small values of h_1 occurring below room temperature. This method is depicted by Fig. 2(a). The sample was bonded between two plates; a metal plate serving as a support and an aluminum-plated silica disk serving as one plate of a parallel plate capacitor. The other capacitor plate was one face of a Be-Cu ring which was placed around the sample. The capacitor was, then, part of a free-running Hartley oscillator, whose frequency was monitored by an electronic counter. For small changes in length, the magnetostriction is simply proportional to the change in frequency of the oscillator. Taking into account the distributed capacity of the leads, C_d , the magnetostriction is given by

$$\frac{\delta l}{l} = \frac{2\epsilon A}{L} \frac{1 + (C_d/C_p)}{C_p} \frac{\Delta f}{f}, \quad (13)$$

where ϵ is the permittivity of free space, A the area of the capacitor plates, C_p the value of the capacity, L the length of the sample, f the frequency of the oscillator, and Δf the change in frequency with strain. At a frequency of 5 Mc/sec, a strain of 10^{-7} produces an easily detectable frequency shift of ~ 10 cps. This method has the advantages of eliminating the problem of magnetoresistance of the strain gauges and variation of gauge factor with temperature, while still permitting the investigator to use relatively small samples. Room-temperature values of the magnetostriction as a function of magnetic field are shown in Fig. 3, for the field parallel and perpendicular to the measurement direction, and for the measurement direction along the [001] and [110]. Saturation occurs below 2 kG, after which a small volume magnetostriction is observed. The values

of h_1 and h_2 , to second degree in the magnetization direction cosines, are given by

$$\left(\frac{\delta l(\theta)}{l}\right)_1 - \left(\frac{\delta l(0)}{l}\right)_1 = -h_1 \sin^2 \theta, \quad (14)$$

$$\left(\frac{\delta l(\theta)}{l}\right)_2 - \left(\frac{\delta l(0)}{l}\right)_2 = -h_2 \sin^2 \theta,$$

where $[\delta l(\theta)/l]_1$ is the strain along the $[001]$ direction when the magnetic field is rotated in the (110) plane. $[\delta l(\theta)/l]_2$ represents the strain along the $[\bar{1}10]$ direction when rotation is in the (001) plane. Here θ is the angle between the measurement direction and the magnetic field. Although complete symmetric curves of $\sin^2 \theta$ were obtained at room temperatures, only the values of $\delta l(\theta)/l$ for $\theta=0$ and $\theta=\pi/2$ are depicted in Fig. 3.

Room-temperature measurements of h_1 and h_2 were made on two samples, one grown by J. W. Nielson and the other by J. R. Cunningham of the Naval Ordnance Laboratory. The agreement was better than 2%. The saturation magnetostriction, λ_s , of a polycrystal of YIG prepared by Cunningham was -2.22×10^{-6} , which is also within 2% of that calculated from the single-crystal measurements.

The temperature dependences of h_1 and h_2 are shown in Fig. 4. Both coefficients are small and negative. The quantity $-h_2$ is larger than $-h_1$ and decreases monotonically from about 8×10^{-6} at liquid nitrogen temperature to about 2×10^{-6} at 450°K. The coefficient $-h_1$ peaks near room temperature with a value of 2.1×10^{-6} . All higher degree coefficients have been found to be less than 5% of h_1 and h_2 at room temperature.

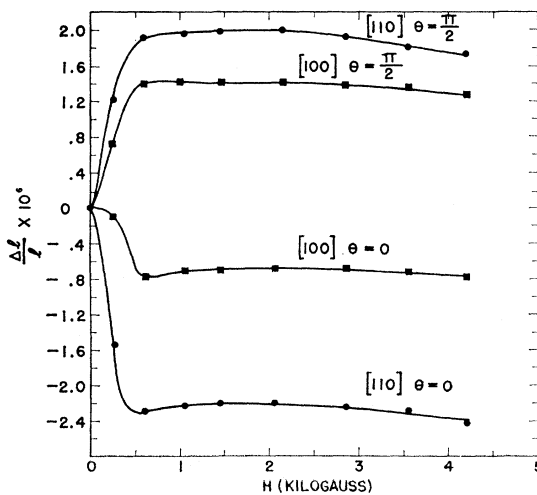


FIG. 3. Field dependence of the magnetostriction of yttrium iron garnet at room temperature. The curves show the changes in length along the $[100]$ and $[110]$ directions, for the magnetic field parallel ($\theta=0$) and perpendicular ($\theta=\pi/2$) to the measurement directions.

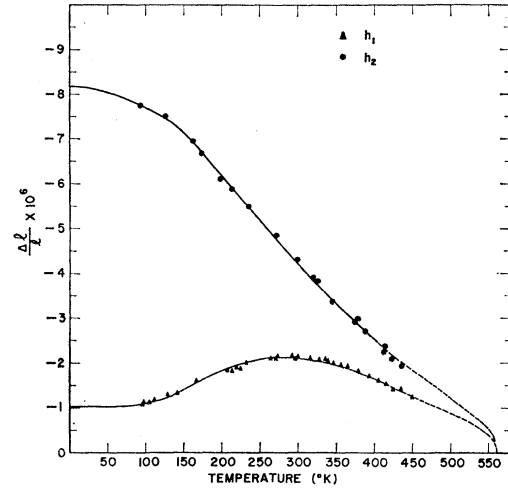


FIG. 4. Magnetostriction of single-crystal yttrium iron garnet as a function of temperature. The calculated curves, shown by the solid lines, are based on sublattice magnetization data of Roberts (reference 9). Dashed lines result from extrapolation of his data.

III. ANALYSIS AND DISCUSSION

To compare our measurements of $h_1(T)$ and $h_2(T)$ to the theoretical equations (11) and (9), we require the temperature dependences of the sublattice magnetizations and of the elastic constants. To our knowledge, the latter have been measured only at room temperature,⁸ but it is to be expected that the elastic constants vary by at most a few percent between 450°K and absolute zero, and, hence, we neglect this variation and employ the room-temperature values.

Roberts⁹ has determined the YIG sublattice magnetizations^{10,11} from liquid-helium temperature up to 400°K by means of nuclear magnetic resonance. To compare theory and experiment it remains only to substitute the sublattice magnetization data at each temperature into the functional dependence of the reduced hyperbolic Bessel function $\hat{I}_{5/2}(\mathcal{L}^{-1}(m_0))$ illustrated in Fig. 1, and to adjust the two magnetoelastic coupling coefficients (one for each sublattice). Letting a refer to the octahedrally coordinated sublattice and d to the tetrahedrally surrounded ions, the coupling coefficients arrived at in this fashion are

$$B_{0,2}^{\gamma}(a) = -9.70 \times 10^6 \text{ ergs/cm}^3, \quad B_{0,2}^{\gamma}(d) = 8.95 \times 10^6 \text{ ergs/cm}^3, \quad (15)$$

$$B_{0,2}^{\epsilon}(a) = 5.67 \times 10^6 \text{ ergs/cm}^3, \quad B_{0,2}^{\epsilon}(d) = -17.2 \times 10^6 \text{ ergs/cm}^3.$$

This choice of coefficients yields the solid curves of

⁸ A. E. Clark and R. E. Strakna, J. Appl. Phys. **32**, 1172 (1961).
⁹ C. Roberts, Compt. Rend. **251**, 2684 (1960).

¹⁰ The sublattice magnetizations of YIG have also been estimated by R. Pauthenet, Ann. Phys. (Paris) **3**, 424 (1958) by means of his magnetization measurements and the Néel theory.

¹¹ deI. Solomon, Compt. Rend. **251**, 2675 (1960) reports room-temperature values by Mössbauer measurements.

Fig. 4. The dashed line extensions are based upon an extrapolation of the sublattice data of Roberts up to a Curie temperature of 560°K. It will be seen that the classical approximation, Eq. (8), is satisfactory. This is to be expected in the case of YIG, in which both magnetic sublattices are populated by $\text{Fe}^{3+} \text{ } ^6S_{5/2}$ ions. Because of the high multiplicity of the iron ion there is little distinction between quantum and classical averages. This classical approximation is, of course, convenient but peripheral to the theory, and for a spin of lower multiplicity one could calculate the dynamical expectation value of \mathcal{Y}_l^0 , the spherical tensor of degree l and order zero, with respect to the Brillouin internal field distribution function, or for any other appropriate model.

The array of magnetoelastic coupling coefficients of Eq. (15) is noteworthy. These coefficients, which represent the strain-induced changes in anisotropy energy of octahedral and tetrahedral ions are the fundamental quantities that one would like to compare to the results of an atomic calculation. Unfortunately, no such calculation has yet been performed on a garnet. However, a qualitative comparison can be made to Tsuya's¹² analysis of the magnetostriction of ferrites. In both materials there are octahedrally and tetrahedrally coordinated magnetic ions. In both materials the magnetostriction is small when the magnetic ion is in an S state (as is Fe^{3+}) thereby eliminating spin-orbit coupling in the unperturbed ground state.

A possible mechanism might be the variation of dipole-dipole (or pseudo-dipole-dipole) energy with strain. Tsuya has shown this effect to be of the order of magnitude that we observe in YIG. However, our theory of the temperature dependence assumes a one-ion magnetoelastic perturbation, and the close agreement with experiment tends to strengthen the plausibility of this one-ion assumption. Furthermore, the one-ion model is in agreement with the conclusions of Folen and Rado¹³ and of Geschwind¹⁴ concerning the magnetic anisotropy energy of ferrites. Indeed, the one-ion nature of the magnetic anisotropy implies the same characteristic of the magnetostriction, since the magnetostriction arises from the variation of anisotropy energy with strain.

That the strain potential, the variation with crystal strain of the electrostatic energy of an ion, plays an essential role in determining the atomic magnetoelastic coupling coefficients is suggested by the comparison of our phenomenological coefficients of Eq. (15) and the second degree strain potential constants, $\rho^{(2)}$, calculated

by Tsuya for the spinel. Tsuya gives:

	Octahedral (b) sites	Tetrahedral (a) sites	
Γ_γ	$\rho_{100}^{(2)} = -\frac{27}{5}WD,$	$\rho_{100}^{(2)} = \frac{8 \times 6}{5(3)^{1/2}}WD,$	(16)
Γ_ϵ	$\rho_{111}^{(2)} = \frac{36}{5}WD,$	$\rho_{111}^{(2)} = -\frac{8 \times 16}{15(3)^{1/2}}WD.$	

Here W and D are crystal field splitting parameters. It will be noted that Tsuya's array of constants displays the same sign variation as our magnetoelastic coefficients, though the actual magnitudes differ, even after correction of our coefficients for the relative populations (24 tetrahedral, 16 octahedral sites per unit cell). The strain potential is, of course, to be combined with some perturbative term quadratic in the spin operators, such as spin-orbit coupling to second order, or intra- or interatomic spin-spin interaction to first order, to produce the magnetoelastic spin Hamiltonian our theory presupposes. It is mentioned incidentally that the relationships between our magnetoelastic coefficients and those of Becker and Döring¹⁵ are

$$B_{0,2}^\gamma(a) + B_{0,2}^\gamma(d) = -\frac{2(4\pi)^{1/2}}{15}b_1(0^\circ\text{K}), \quad (17)$$

$$B_{0,2}^\epsilon(a) + B_{0,2}^\epsilon(d) = -\left(\frac{4\pi}{15}\right)^{1/2}b_2(0^\circ\text{K}).$$

It is informative to compare our measurements to reported values of static magnetostriction and of dynamic acoustic wave rotation and resonance. The only published data of the static magnetostriction we find are the polycrystal measurements of Nakamura and Siguira.¹⁶ While our suitably averaged ($\lambda_s = \frac{2}{3}\lambda_{100} + \frac{1}{3}\lambda_{111}$) single-crystal values agree within 2% with our own polycrystal measurements on several samples of different origin, these values all differ markedly from those of Nakamura and Siguira. These authors report a room temperature $\lambda_s = 0.37 \times 10^{-6}$, which is far outside our experimental uncertainty of $\pm 5\%$.

On the other hand, the magnetoelastic coupling coefficients we derive from our magnetostriction measurements do agree reasonably well with the results of several dynamic measurements. To make this comparison at any temperature we average the effective coupling coefficients for the sublattices at that temperature. For while our theory allows of a separation into the individual sublattice magnetoelastic coupling coefficients other investigators report only macroscopic averages.

In an acoustic wave rotation experiment at 500

¹² N. Tsuya, Sci. Repts. Research Insts. Tohoku Univ. Ser. B 8, 161 (1957).

¹³ V. J. Folen and G. T. Rado, J. Appl. Phys. 29, 438 (1958).

¹⁴ S. Geschwind, Phys. Rev. 121, 363 (1961).

¹⁵ R. Becker and W. Döring, *Ferromagnetismus* (Julius Springer-Verlag, Berlin, 1939) p. 136.

¹⁶ A. Nakamura and Y. Siguira, J. Phys. Soc. Japan 15, 1704 (1960).

Mc/sec, Matthews and LeCraw¹⁷ measure an average coupling coefficient at room temperature of $\bar{B}^\epsilon = -6.8 \times 10^6$ ergs/cm³, while Hall and Bailey¹⁷ find $\bar{B}^\epsilon = -3.7 \times 10^6$ ergs/cm³. Evaluating the room-temperature sublattice magnetizations from the data of Roberts,⁹ we arrive at the basis of our data at

$$\begin{aligned} \bar{B}^\epsilon &= B_{0,2}^\epsilon(a) \hat{I}_{5/2}(\mathcal{L}^{-1}(m_a)) + B_{0,2}^\epsilon(d) \hat{I}_{5/2}(\mathcal{L}^{-1}(m_d)) \\ &= -5.85 \times 10^6 \text{ ergs/cm}^3. \end{aligned} \quad (18)$$

It is only the Γ_ϵ strains which are excited in the shear wave rotation experiments; this technique does not yield the average Γ_γ magnetoelastic coefficient.

However, we can compare our Γ_γ data by consideration of the determination of the macroscopic coefficients recently made by Smith and Jones,¹⁸ who measure the shift in magnetic field for resonance with sample strain. A uniaxial stress is applied along the [110] direction, and the shift in field for resonance measured along the [100] and [110] axes. In this fashion the authors can determine both the average Γ_γ and Γ_ϵ coefficients. They report that at room temperature $\bar{B}^\gamma = -1.65 \times 10^6$ ergs/cm³, $\bar{B}^\epsilon = -6.37 \times 10^6$ ergs/cm³. The Γ_γ coefficient of Smith and Jones is in very close agreement with our value of

$$\begin{aligned} \bar{B}^\gamma &= B_{0,2}^\gamma(a) \hat{I}_{5/2}(\mathcal{L}^{-1}(m_a)) + B_{0,2}^\gamma(d) \hat{I}_{5/2}(\mathcal{L}^{-1}(m_d)) \\ &= -1.6 \times 10^6 \text{ ergs/cm}^3. \end{aligned} \quad (19)$$

Furthermore, it is seen that their Γ_ϵ coefficient agrees rather well with our value, as given in Eq. (18).

Yet another technique in the investigation of magnetoelastic coupling has been employed by Turner¹⁹

¹⁷ H. Matthews and R. C. LeCraw, Phys. Rev. Letters **8**, 397 (1962).

¹⁸ A. B. Smith and R. V. Jones, J. Appl. Phys. Suppl. **34**, 1283 (1963).

¹⁹ E. H. Turner, *Advances in Quantum Electronics* (Columbia University Press, New York, 1961), p. 427.

and by Olson.²⁰ In this experiment one observes the dependence of onset of instability with increasing rf power as a function of steady dc field, in parallel pumping ferromagnetic resonance. The onset of instability is suppressed by the coupling of spin waves to phonons. The values of \bar{B}^ϵ reported by Turner and by Olson are again within the range of those measured by other means. Olson, however, attempts to relate the measured magnetoelastic coefficient to the theory of the temperature dependence of a ferromagnetic model. Olson invokes both the lowest degree shear coefficient, $B_{0,2}^\epsilon$, and a fourth-degree coefficient $B_{0,4}^\epsilon$ which he evaluates as 1.6 times as large as $B_{0,2}^\epsilon$ and of opposite sign. As we have mentioned, our data show that any higher degree coefficients, of either Γ_ϵ or Γ_γ type, are at most 5% of the $l=2$ coefficients at room temperature [or, on the basis of the $l(l+1)/2$ power law, are less than 10% at 0°K.]

As a final comment, it is interesting that, although each sublattice has a monotonically decreasing magnetization (with increasing temperature) and that the hyperbolic Bessel functions are monotonic functions of their argument, the crystal magnetostriction can display a maximum. This can come about if, as in the case of h_1 in YIG, the two sublattice coupling coefficients are of opposite sign (and comparable magnitude) and the coefficient of smaller magnitude is associated with the sublattice whose reduced magnetization decreases more rapidly with increasing temperature. That is, for YIG, $|B_{0,2}^\gamma(d)| < |B_{0,2}^\gamma(a)|$ and Roberts data shows that $m_d(T)/m_d(0) \equiv m_d$ decreases with increasing temperature more rapidly than does m_a .

Indeed, if the coefficient of larger magnitude (but opposite sign) is associated with the faster decreasing magnetization, the material could display a magnetostriction compensation point even in the absence of a magnetization compensation point.

²⁰ F. O. Olson, Suppl. J. Appl. Phys. **34**, 1281 (1963).